Effect of Alternating Stray Current and Stress on the Corrosion Behavior of X80 Pipeline Steel in Soil Simulated Solution

Xinhua Wang, Xuting Song, Yingchun Chen[*], Zuquan Wang

College of Mechanical Engineering and Applied Electronics Technology, Beijing University of Technology, Beijing 100124, China
[*]E-mail: ychen08089@163.com

The corrosion behavior of X80 pipeline steel in 3.5 wt.% NaCl solution and simulated Dagang soil solution under different alternating current (AC) electrical densities was studied using the weight loss method, and was tested and analyzed using the electrochemical test technique and surface analysis technique, such as open circuit potential (OCP), polarization curve and scanning electron microscopy (SEM). The results showed that the corrosion potential of X80 pipeline steel was negative under the coupling of AC and stress. With the increase of AC stray current density, the negative shifted rate of corrosion potential increased, which indicated that the electrochemical corrosion behavior of X80 pipeline steel aggravated due to the coupling of AC stray and stress. In addition, the coupling of AC stray current and stress affected the corrosion process of X80 pipeline steel, which did not show any tendency of passivation in the experimental. Under the action of the alternating stray current, the reduction reaction of H_2 and O_2 occurred in X80 pipeline steel in the solutions of 3.5% NaCl and Dagang soil. When the applied stress was kept constant, the corrosion morphology of X80 pipeline steel samples underwent uniform corrosion under low AC stray current density (0 - 100 A/m^2), whereas the corrosion morphology of X80 pipeline steel samples showed that the pitting corrosion occurred under the action of high AC stray current density (100 - 300 A/m^2).

1. INTRODUCTION

The pipeline, known as the lifeline of the country, has an important strategic position in the national economy [1,2]. Therefore, the safety of the pipeline's operation is particularly important. However, with the rapid construction of high-voltage transmission lines and electrified railways, the risk of pipe exposure to stray currents increases [3-5]. Stray current interference causes corrosion of

the pipelines and accelerates its destruction [6-7]. Over time, the stray current interference has become a serious threat to the normal operation of oil and gas pipelines. Stray current is different from the regular current path, due to which, it is one of the major reasons for the corrosion and leakage of metal pipes. It is also worth mentioning that corrosion is the main cause of pipeline failures. The accidents due to the rupture of pipelines caused by corrosion occur on average every six months, whereas the corrosion damage to pipelines due to stray currents (DC and AC stray currents) and stress is gaining increasing attention [8-12].

The study of AC stray current corrosion is mainly based on the electrochemical theory. Some pioneering works [13] argue that the effect of alternating stray current on the corrosion of metal is caused by its depolarization of anodic and cathodic reactions and the weakening of the electrochemical bluntness of the metal.

Bockris and Reddy [14] argued that AC corrosion is mainly caused by the asymmetry of anodic and cathodic Tafel slope. In 1994, Lalvani and Lin [15] theoretically studied for the first time the change in corrosion potential and corrosion current density under the action of AC by applying the Tafel equation. In 1998, on the basis of Lalvani's work Bosch and Bogaerts [16] studied the theoretical model of the electrochemical process controlled by the activation and diffusion of the cathodic process. The modified Bessel equation was used to further study the corrosion behavior of metal under different current densities. Later, Zhang [17] characterized the corrosion behavior under the action of AC by using the perturbation method, which considered the polarization impedance, double layer capacitance and solution resistance. Recently, Li [18] conducted an experimental study on the corrosion behavior of X70 pipeline steel in the marine environment under the action of alternating stray current, and theoretically studied the corrosion mechanism.

In-depth literature studies show that current research on AC or DC stray current corrosion is based on the buried pipeline steel under pressure, whereas the factors affecting the corrosion process are studied individually. There is no study focusing on the coupling of a variety of factors, and studying their effect on the corrosion of pipeline steel. However, the pipeline steel, especially the high-strength pipeline steel, inevitably undergoes elasto-plastic deformation under stress, such as residual stress and working pressure, which has an important influence on the thermodynamics and kinetics of high-strength steel pipelines corrosion. Boven, Rogge and Chen [19] found that both residual stress and applied stress can accelerate the corrosion behavior of near neutral NS_4 simulation solution of X65 pipeline steel, promote the formation of corrosion pits and accelerate the corrosion rate. Xu and Cheng [20] considered that the static elastic stress exerted on the pipeline steel has a limited influence on its corrosion, while when plastic strain is applied, the pores of the pipeline steel will increase and the activity of apparel will be enhanced.

In the transport process of the high-pressure medium, high-strength steel pipeline undergoes some inevitable stress effects, which have great influence on the thermodynamics and kinetics of high-strength steel pipeline corrosion. The study of corrosion mechanism and corrosion behavior of high strength steel pipeline under the coupling effect of stray current and stress is a recent problem, which is faced in the process of use, promotion and long-term safety of the high strength steel pipeline. In this paper, the corrosion behavior of X80 pipeline steel under the coupling of stress and alternating stray current was studied in 3.5 wt.% NaCl solution and Dagang soil simulated solution. The techniques

used for the analysis consisted of open-circuit potential (OCP), polarization curve, and scanning electron microscopy (SEM).

2. EXPERIMENTAL

2.1 Materials and the test solutions

The test material used in the test is a smooth plate-like X80 steel tensile specimen, the dimensions of which are shown in Figure 1. X80 pipeline steel is mainly composed of ferrite, acicular ferrite and flaky bainite, whereas the main chemical composition of the X80 pipeline steel specimen is presented in Table 1. The yield strength ($\sigma_{0.2}$), tensile strength (σ_b), and yield ratio ($\sigma_{0.2}/\sigma_b$) of X80 steel have values of 552 MPa (Ys), 705 MPa and 0.79 respectively. The axial direction of the specimen, which is along the radial direction of the actual pipe, ensures that the direction of the main force of the tensile specimen is the same as that of the actual direction of the pipe.
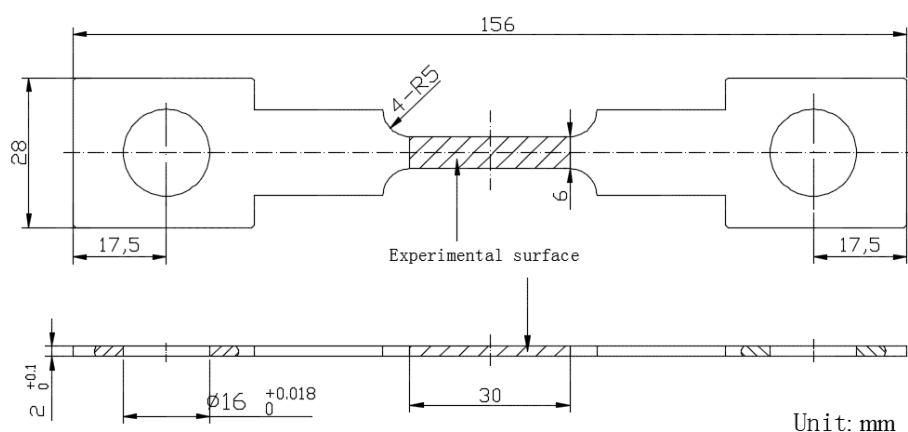

Figure 1. Dimensions of the X80 pipeline steel sample

Table 1. Chemical composition of the X80 pipeline steel (wt.%)

Pipeline grade	C	Si	Mn	P	S	Nb	Ti	other
X80	0.060	0.216	1.80	0.0137	0.0009	0.105	0.013	Mo, Ni, Cu, Cr

Before the experiment, the working surface of the sample was polished using 60# - 1500# grade with SiC water sandpaper. Later, the sample was washed with anhydrous ethanol and deionized water, dried and placed in the drying oven.

The test solution used in this research is Dagang simulated soil solution, which is a typical acidic soil solution in the marine environment (PH = 8.3). The ionic concentration and chemical composition of Dagang simulated solution are shown in Tables 2 and 3. As a comparison, tests were

operated in 3.5% NaCl solution as well, which is a typical neutral electrolyte solution in laboratory tests.

Table 2. Ion concentration of Dagang simulated soil solution (g / L)

NO_3^{2-}	Cl^-	SO_4^{2-}	HCO_3^-	Ca^{2+}	Mg^{2+}	K^+	Na^+
0.188	15.854	2.04	0.181	0.378	0.643	0.225	9.982

Table 3. Chemical composition of Dagang simulated soil solution (g)

$CaCl_2$	NaCl	$MgSO_4 \cdot 7H_2O$	KNO_3	$NaHCO_3$
1.049	25.020	5.228	0.306	0.249

2.2. Electrochemical test

In the immersion test, SG1005•5 MHz digital synthesis signal generator was used to produce different densities of AC stray current (30 A/m^2, 100 A/m^2, 200 A/m^2, and 300 A/m^2). RGM-6050 microcomputer controlled electronic slow stress corrosion testing machine was used to exert a force equal to the 30% yield stress of X80 steel samples (165.6 MPa). The soaking experiment was conducted for 24h. After the experiment finished, the sample was removed to observe the morphology, and then placed back into the rust (0.5g Sb_2O_3 + 1.5g $SnCl_2$ • $2H_2O$ + 25ml HCl). The samples were cleaned with deionized water until the corrosion products on the surface of the X80 steel were completely removed. After being sufficiently dried, the samples were observed using an S-3400N ll (Hitachi, Japan) type scanning electron microscope.

In this paper, Princeton's PARSTAT2273 electrochemical workstation was used to test the open-circuit potential and the polarization curves of X80 pipeline steel. The electrochemical test of the pipeline steel, under the combined action of AC and stress, is shown in Figure 2. The experiment uses a three electrode system, in which the working electrode is the X80 steel (working area is 1 cm^2), saturated calomel is the reference electrode, and platinum is the auxiliary electrode. One end of the AC signal generator is connected to the X80 steel sample, whereas the other is connected to the graphite electrode. Capacitance (500 µF) is used to prevent the electrochemical test system from interfering with the AC power supply, while the inductance (15 H) is used to prevent the AC from interfering with the electrochemical test system, ensuring that the two circuits are independent of each other. After stewing solution for one hour when the AC stray current is applied, the process of measuring the open circuit potential was initiated. Under the action of AC, the polarization curve was tested until the open-circuit potential was measured for 30 minutes. The polarization curve was obtained using the Tafel test. Its scanning rate was 1 mV/s, and the scanning potential was -0.5 - 0.7 V. Finally, the experimental data were analyzed using the Origin Pro software.

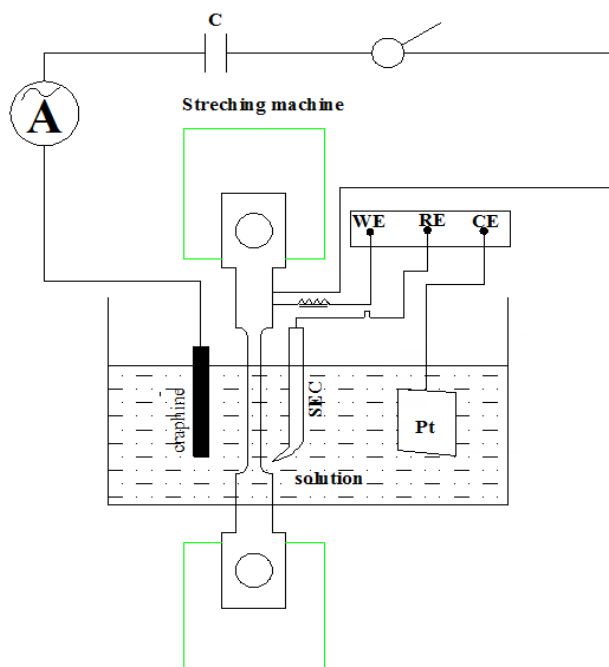**Figure 2.** Schematic of the experimental device used to study the combined effect of AC and stress

3. RESULTS AND DISCUSSION

3.1 Electrochemical test results

Figure 3 shows the open circuit potential of X80 pipeline steel in 3.5% NaCl solution and Dagang soil simulated solution under the effect of stress and AC stray current with different densities. It can be seen from figure 3(a) that the open-circuit potential of X80 pipeline steel in 3.5% NaCl solution was -0.66 V under the stress of 165.6 MPa. When the applied stress was kept constant and the electrical density of AC was increased to 30 A/m^2, the open circuit potential of X80 pipeline steel changed to -0.72 V, whereas the negative shift amplitude also became larger. Similarly, when the applied stress was kept constant, and the electrical density of applied AC was sequentially increased to 100 A/m^2, 200 A/m^2, and 300 A/m^2, the open circuit potential of X80 pipeline steel in 3.5% NaCl solution changed to -0.75 V, -0.78 V, and -0.80 V, respectively. From figure 3(b), it can be seen that, under the action of 165.6 MPa stress, the open circuit potential of X80 pipeline steel in Dagang solution was -0.72V. When the magnitude of stress was kept constant and the electrical density of applied AC was sequentially increased to 30 A/m^2, 100 A/m^2, 200 A/m^2, and 300 A/m^2, the open circuit potential of X80 pipeline steel in Dagang solution changed to -0.82 V, -0.88 V, -0.91V, and -0.97 V, respectively. Under the combined effect of stress and AC, the corrosion potential decreased, indicating that the X80 pipeline steel showed an increased tendency to corrode. This is a good agreement with other researchers [21, 22].
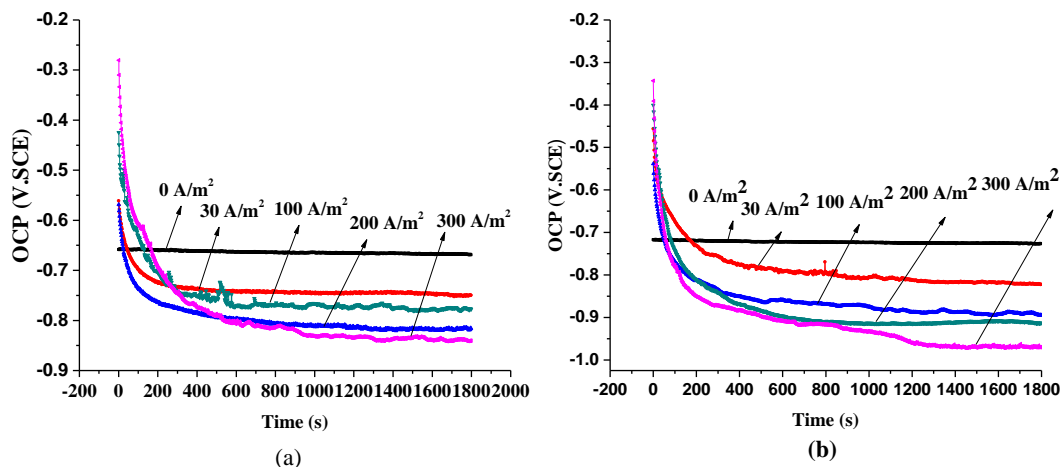
Figure 3. OCP curves of X80 steel at different AC stray current densities in (a) 3.5% NaCl solution (b) Da gang simulated soil solution

Figure 4 shows the polarization curves of X80 pipeline steel in 3.5% NaCl solution and Dagang solution under the combined effect of 165.6 MPa stress and AC. It can be seen that under certain stress conditions, With the increase of AC stray current density, the corrosion potential became negative, whereas the offset gradually became smaller and smaller. In addition, the corrosion current density also increased with the increase of AC stray current density. Under the action of stress and AC, the Tafel slopes of anode and cathode of X80 pipeline steel changed. The influence of AC and stress on the anode's polarization process was more significant than that on the cathode's polarization. However, the cathode's current density increased with the increase in AC's electrical density. From the polarization curve shown in figure 4, it can be seen that the coupling of stress and AC accelerates the corrosion of X80 pipeline steel.
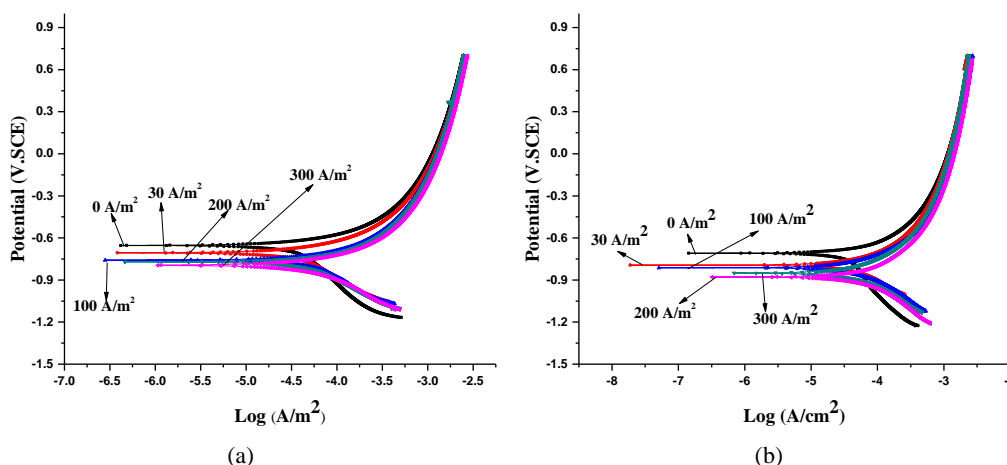

Figure 4. Polarization curves of X80 steel at different AC stray current densities in (a) 3.5% NaCl solution (b) Da gang simulated soil solution

The kinetic parameters in tables 4 and 5 are obtained by fitting the polarization curves in Figure 5, including the AC density anode's Tafel slope b_a and cathode's Tafel slope b_c, and the fitting is performed according to the literature [23]. From these, it can be seen that the anode's Tafel slope b_a and cathode's Tafel slope b_c changed due to the influence of AC and stress. Comparing the data presented in Tables 5 and 6, it can be seen that the coupling of AC and stress has a significant influence on the polarization of anode. Figure 4, Table 4 and Table 5 show that, with the increase in AC and stress, the corrosion potential of the metal changed.

Lalvani and Goidanich [24, 25] put forward that under the interference of AC power applied, the corrosion potential of metal is shifted, and the direction of corrosion potential offset is related to absolute ratio r (given by b_a/b_c) of the Tafel slope of anode and cathode. With the increase in AC's electrical density, the ratio r increased, which was used to measure the offset of the corrosion potential. When $r = 1$, the corrosion potential did not change, whereas when r was close to 1, the offset was smaller. When $r < 1$ or $r > 1$, the corrosion potential will be shifted to negative or positive. The results also showed that with the increase in AC's electrical density, r attained a value closer to 1, whereas the offset in corrosion potential became smaller, which was the same as that seen in Figure 4.

Table 4. Electrochemical parameters of X80 pipeline steel in 3.5% NaCl solution under a stress of 165.6 MPa and different AC's densities

i (A/m^2)	i_{corr} (A/cm^2)	b_a (mV)	b_c (mV)	b_a/b_c
0	1.5×10^{-5}	120.1	924.1	0.1
30	5.1×10^{-5}	145.7	331.1	0.4
100	7.8×10^{-5}	178.9	380.7	0.5
200	1.2×10^{-4}	286.4	485.4	0.6
300	1.3×10^{-4}	294.0	381.9	0.8

Table 5. Electrochemical parameters of X80 pipeline steel in Dagang solution under the effect of 165.6 MPa stress and different AC's electrical densities

i (A/m^2)	i_{corr} (A/cm^2)	b_a (mV)	b_c (mV)	b_a/b_c
0	1.6×10^{-5}	142.4	593.4	0.2
30	5.3×10^{-5}	156.3	274.3	0.6
100	8.1×10^{-5}	197.0	298.6	0.7
200	1.4×10^{-4}	244.6	344.5	0.7
300	1.7×10^{-4}	289.0	352.5	0.8

3.2 Corrosion rate calculation

The corrosion rate is calculated by weight loss method, and the corrosion electrochemical equivalent is calculated by the Equations (1), (2)

$$\Delta W = W_0 - W \qquad \text{（1）}$$
$$V_{corr} = \Delta W / St \qquad \text{（2）}$$

Where ΔW —— The average weight loss of the sample, g;

W_0 —— The original weight of the sample, g;

W —— Remove the corrosive product after the sample weight, g;

S —— The working area of the sample, m^2;

t —— Soaking time, h;

V_{corr} —— Corrosion rate，g/(m^2·h)

Figure 5 shows the corrosion rate of X80 pipeline steel in 3.5% NaCl solution and Dagang solution under the combined action of stress and AC. It can be seen that, for a certain stress, with the increase in AC's electrical density, the corrosion rate of X80 pipeline steel increased. When the applied stress and AC's electrical density were 165.6MPa and 30 A/m^2, respectively, the corrosion rate of X80 steel in 3.5% NaCl solution was about 2.73 times of that with no AC interference. When the applied stress and AC's electrical density were 165.6 MPa and 300 A/m^2, respectively, the corrosion rate of X80 pipeline steel was as high as 1.09 mm/a. The corrosion rate of X80 pipeline steel in Dagang solution under different AC stray current densities and stress was not much different from that in 3.5% NaCl solution. The impact of stress on the corrosion of oil and gas pipeline was small, whereas the impact of AC on the corrosion of oil and gas pipeline was relatively more significant.
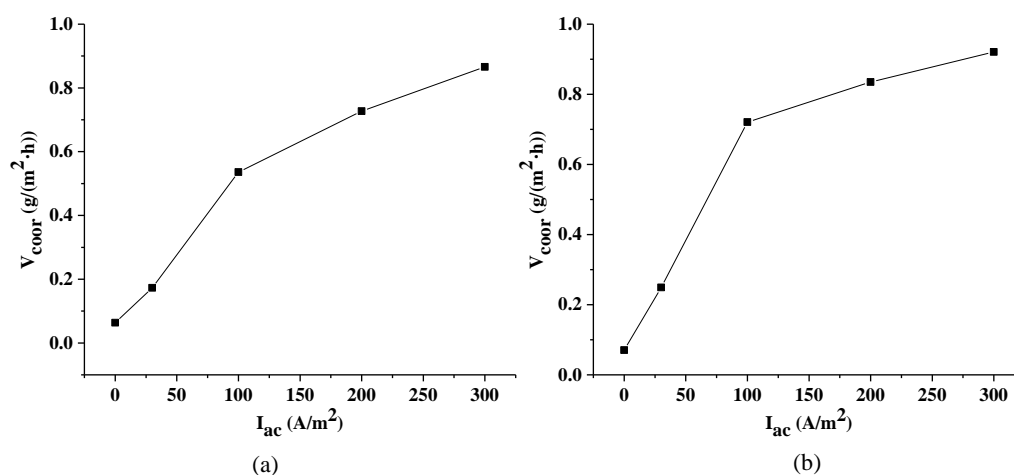

(a)   (b)

Figure 5. Corrosion rate of X80 pipeline steel at different AC stray current densities in (a) 3.5% NaCl solution (b) Da gang simulated soil solution

3.3 Analysis of corrosion morphology

Figures 6 and 7 show the macroscopic morphology of corroded X80 pipeline steel, which was immersed in 3.5% NaCl solution and Dagang solution for 24 h under the coupling effect with a 165.6 MPa tensile stress at various AC current density.

It can be seen that, under a certain pressure, the corrosion degree of X80 pipeline steel increased with the increase of AC current density for the same soaking time. In addition, with the passage of time, the accumulation of corrosion products resulted in a thicker layer. It can be seen from

Figures 6(a) and 7(a) that the outer layer of X80 pipeline steel was mainly composed of brown-red products, whereas the corrosion products were smaller in quantity when the applied stress was 165.6MPa. Under the action of high AC electrical density (100 - 300 A/m^2), the outer brown and reddish brown matter increased in quantity, and the black product became more obvious. Meanwhile, the thickness of the corrosion product also increased. The macroscopic morphology of corroded X80 pipeline steel under the coupling of AC and stress was similar in both the 3.5% NaCl solution and the Dagang soil solution.
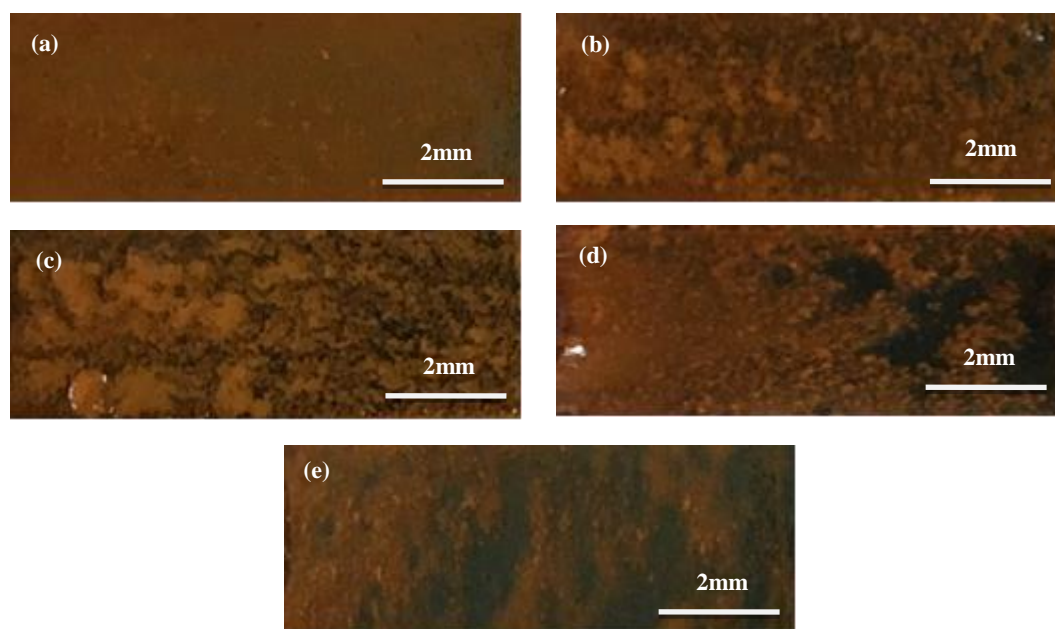

Figure 6. corrosion morphology of X80 steel samples in 3.5%NaCl solution at different AC stray current densities (A) 0A/m^2, (B) 30A/m^2, (C) 100A/m^2, (D) 200A/m^2, and (E) 300A/m^2
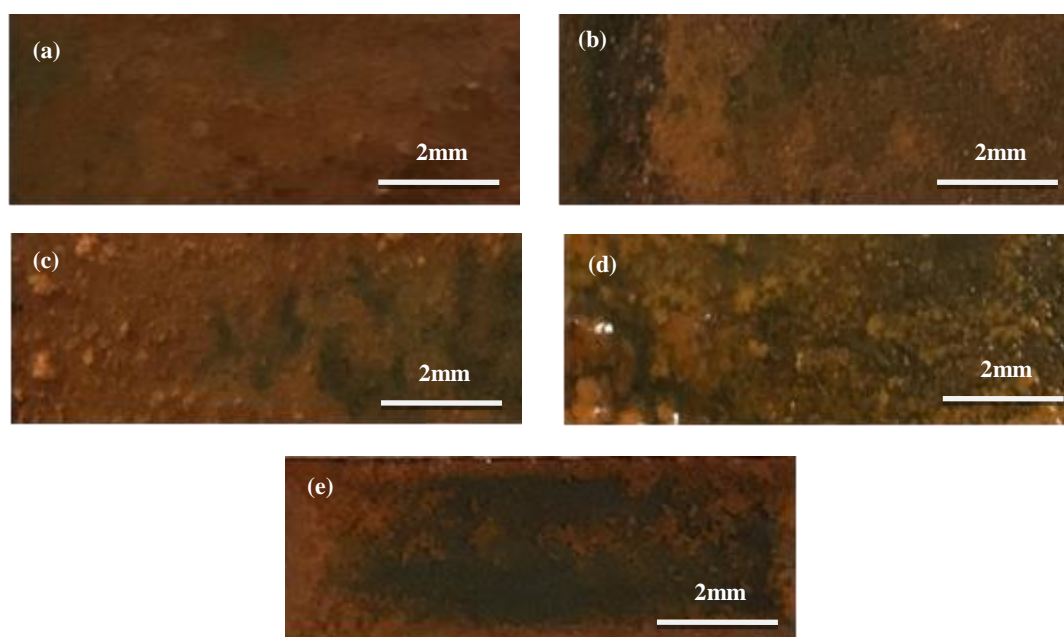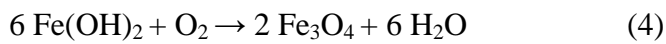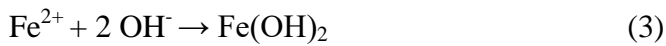

Figure 7. corrosion morphology of X80 steel samples in Dagang solution at different AC stray current densities (A) 0A/m^2, (B) 30A/m^2, (C) 100A/m^2, (D) 200A/m^2, and (E) 300A/m^2

Under the action of AC, the corrosion products of X80 steel are mainly composed of $Fe(OH)_2$, FeOOH and Fe_3O_4 [26-28]. X80 steel surface corrosion product accumulation process as shown in Equations (3), (4) and (5)

$$Fe^{2+} + 2\ OH^- \rightarrow Fe(OH)_2 \qquad (3)$$
$$6\ Fe(OH)_2 + O_2 \rightarrow 2\ Fe_3O_4 + 6\ H_2O \qquad (4)$$
$$4\ Fe(OH)_2 + O_2 \rightarrow 4\ FeOOH + 2\ H_2O \qquad (5)$$

Since the direction of AC interference is alternated, the cycle of anodic polarization and cathodic polarization occurs in the pipeline steel. In the positive half cycle of AC interference, anodic polarization occurs on the steel surface to produce Fe^{2+}. Then, Fe^{2+} and OH^- ions combine to form $Fe(OH)_2$ on the electrode surface as shown in Equation (3).

a) 0 A/m^2 b) 30 A/m^2

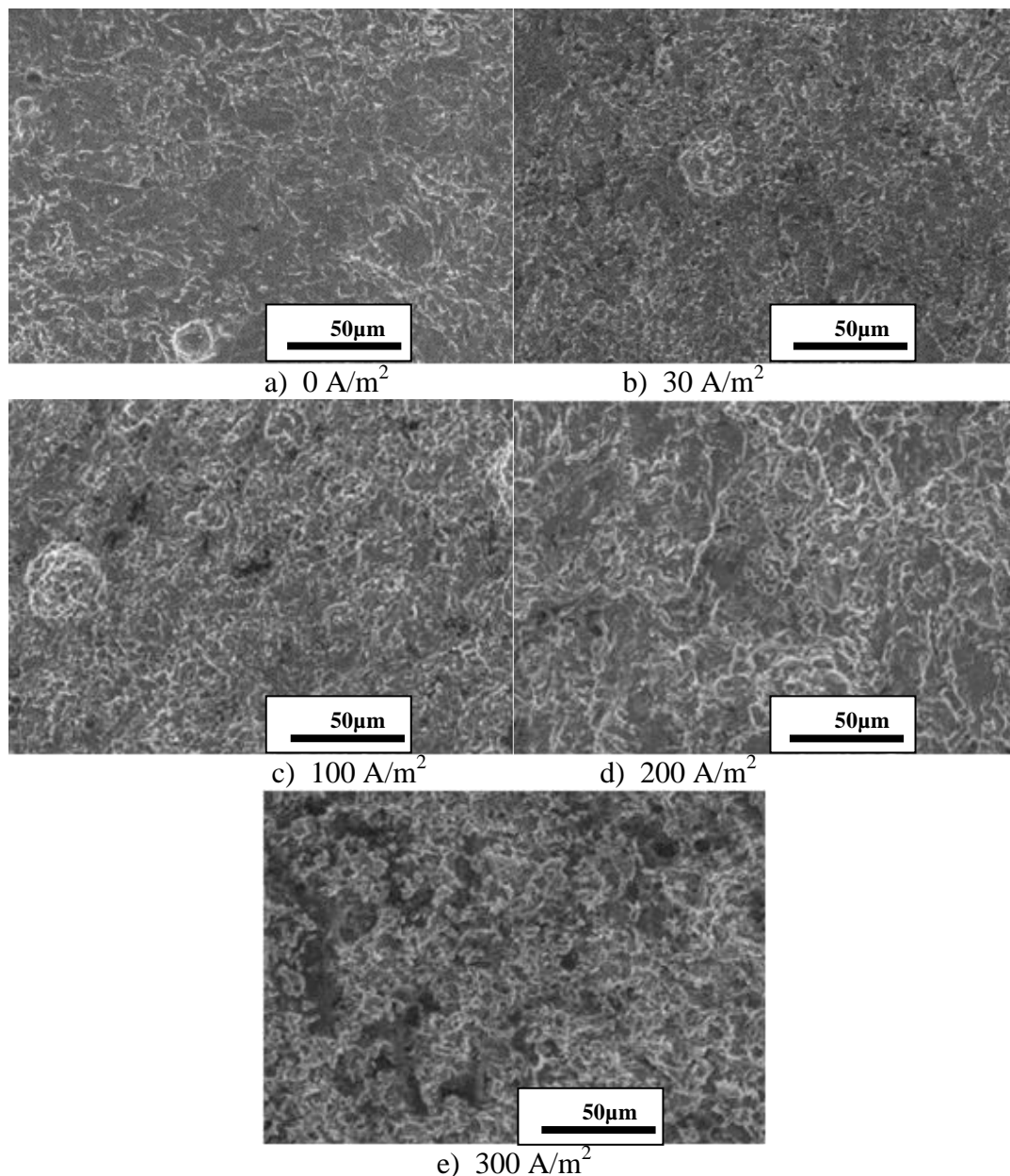c) 100 A/m^2 d) 200 A/m^2

e) 300 A/m^2

Figure 8. Microscopic morphology of X80 pipeline steel in 3.5% NaCl solution under the coupling of 165.6 MPa stress and different electrical densities of AC
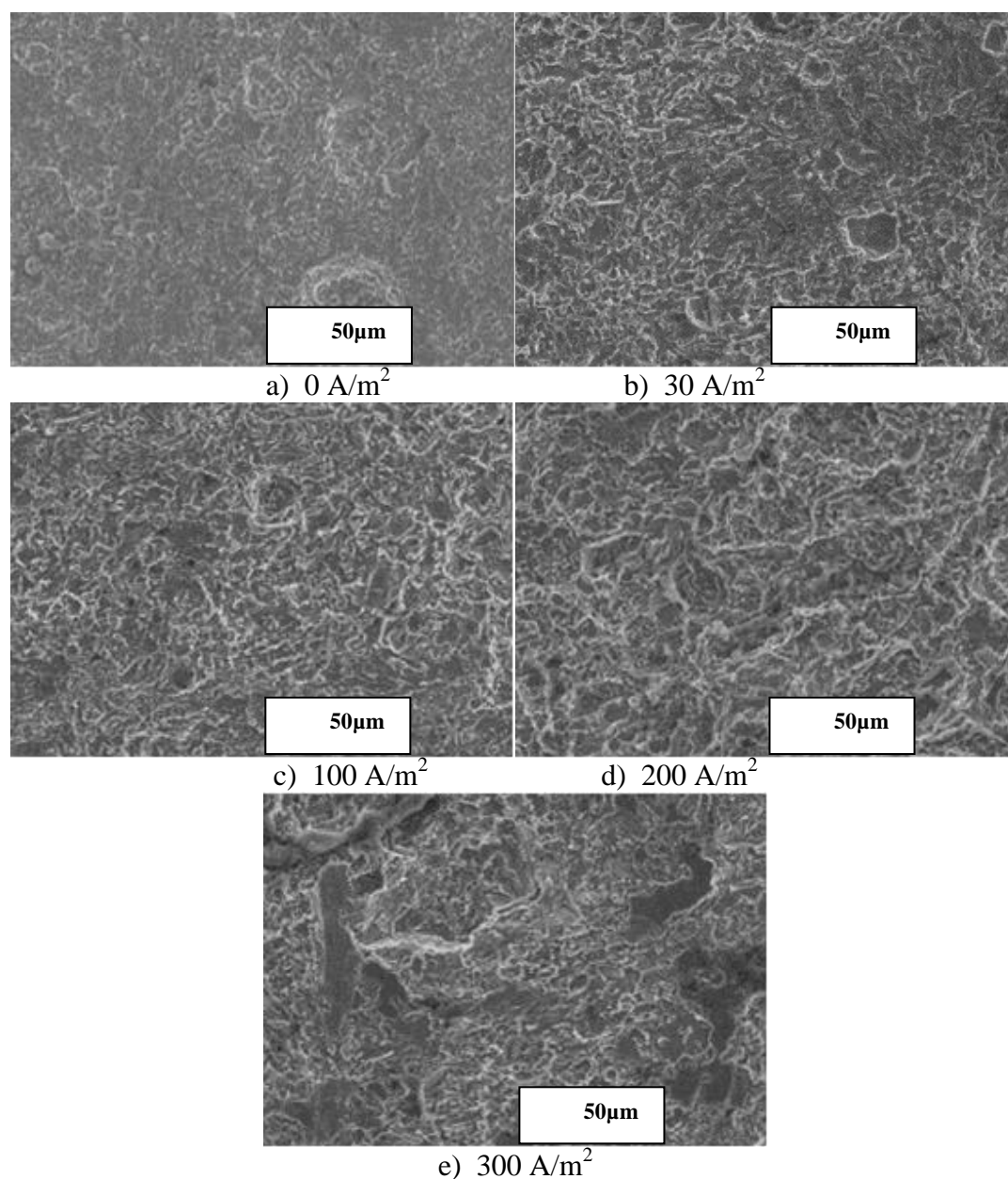
a) 0 A/m^2 b) 30 A/m^2

c) 100 A/m^2 d) 200 A/m^2

e) 300 A/m^2

Figure 9. Microscopic morphology of X80 pipeline steel in Dagang solution under the coupling of 165.6 MPa stress and different electrical densities of AC

However, the structure of Fe (OH)$_2$ is relatively loose and it can be converted to Fe$_3$O$_4$, as shown in equation (4). In the negative half cycle of AC interference, cathodic polarization occurs on the steel surface and Fe$_3$O$_4$ is reduced to Fe(OH)$_2$. As the degree of polarization increases, a portion of Fe(OH)$_2$ continues to be oxidized to Fe$_3$O$_4$ and the other portion becomes FeOOH during the next anodic polarization.

Therefore, under the action of AC, the inner corrosion layer of X80 pipeline steel is black Fe$_3$O$_4$ and the outer corrosion layer is Fe(OH)$_3$. With the corrosion proceeds further, Fe(OH)$_3$ is converted into the relatively loose Fe$_2$O$_3$ and FeOOH. However, the dense Fe$_3$O$_4$ is located in the bottom of the corrosion products, which play a protective role on the tube free steel substrate [29].

Figures 8 and 9 show the microstructure of corrosion products of X80 pipeline steel in 3.5% NaCl solution and Dagang solution under the coupling of 165.6 MPa stress and different electrical densities of AC. Figures 8(a) and 9(a) show that, when the applied stress was 165.6 MPa, the X80 pipeline steel underwent a rather uniform corrosion, whereas a small amount of pitting was also observed on it. For a constant stress, With the increase of AC density, the degree of corrosion of the sample aggravated, and the local corrosion obviously increased such as pitting. At the same time, the surface of X80 pipeline steel became progressively rough, and the originally smooth surface completely corroded. Under the effect of 165.6MPa stress and $300A/m^2$ current density of AC, the pitting on the surface of the specimen was obvious, and small pits combined to form larger pits. This way, the diameter and depth of the corrosion pits increased. The distribution of pits was relatively concentrated, and the circular pits were combined with each other into gully-like pits, causing local corrosion of the sample surface. From Figures 8 and 9, it can be seen that, under the combined action of stress and AC, the corrosion of X80 pipeline steel was more severe than that under the effect of any of the two factors (stress or AC). When the stress was constant, the corrosion of the X80 pipeline steel surface increased with the increase in the electrical density of AC.

4. CONCLUSION

Based on the results, following conclusions are drawn.

(1) Under the coupling of alternating stray current and stress, the corrosion potential of high strength steel specimen (X80 pipeline steel) decreased with the increase in the electrical density of AC. This phenomenon can be reasonably explained by the electrochemical model, indicating that the applied stress and AC interference, will contribute to the corrosion reaction at the thermodynamic level.

(2) Based on the Buchler mechanism, the alternating stray current accelerated the corrosion reaction of high strength steel specimen at the level of chemical reaction kinetics, whereas the stress did not significantly promote the corrosion of X80 pipeline steel sample.

(3) The coupling of alternating stray current and stress changed the corrosion morphology of high strength steel samples. When the stress was constant, the corrosion morphology of X80 steel specimen showed uniform corrosion under the action of low AC density, whereas the corrosion morphology of high strength steel specimen showed pitting corrosion under the influence of high AC density.

References

1. S. K. Sharma and S. Maheshwari, *J. Nat. Gas Sci. Eng.*, 38 (2017) 203.

2. S. D. Koduru and M. A. Nessim, Review of Quantitative Reliability Methods for Onshore Oil and Gas Pipelines, Risk and Reliability Analysis: Theory and Applications, Springer International Publishing, (2017).
3. S. Nesic, *Corros Sci.*, 49 (2007) 4308.
4. G. Jacobson, *Mater. Perform.*, 46 (2007) 26-34.
5. X. Wang, X. Tang and L. Wang, *J. Nat. Gas Sci. Eng.*, 21 (2014) 474.
6. Y. Hosokawa, Overcoming the new threat to pipeline integrity - AC corrosion assessment and its mitigation, 2008.
7. T. H. Matcor, *World Pipelines.*, 12 (2007) 25.
8. I. Ragault, AC Corrosion Induced by V.H.V. Electrical Lines on Polyethylene Coated Steel Gas Pipelines, Proc. Nace International Conference Corrosion, 1998.
9. C. Movley, Pipeline corrosion from induced A.C., NACE Corrosion/2005, Houston TX, USA,2005, Paper No. 05132.
10. H. Hanson and J. Smart, *Corros.*, (2004).
11. L. Lazzari, S. Goidanich and M. Pedeferri and M. Ormellese, Influence of AC on corrosion kinetics for carbon steel, zinc and copper, Corrosion 2005, Paper No. 05189.
12. R. Wakelin and C. Sheldon, Investigation and Mitigation of AC Corrosion on a 300 MM Natural Gas Pipeline, NACE Corrosion/2004, New Orleans LA, USA, 2004, Paper No. 04205.
13. D. T. Chin and J. L. Wendt, *Corros Sci.*, 25 (1985) 889.
14. J. O. M. Bockris and A. K. N. Reddy, Modern Electrochemistry: An Introduction to an Interdisciplinary Research, Macdonal, (1970).
15. S. B. Lalvani and X. Lin, *Corros Sci.* 36 (1994) 1039.
16. R. W. Bosch and W. F. Bogaerts, *Corros Sci.* 40 (1998) 323.
17. R. Zhang, P. R. Vairavanathan and S. B. Lalvani, *Corros. Sci.* 50 (2008) 1664.
18. Y. C. Li, C. Xu, R. H. Zhang, Q. Liu, X. H. Wang and Y. C. Chen, *Int. J. Electrochem. Sci.* 12 (2017) 1829.
19. G. V. Boven, R. Rogge and W. Chen, Residual Stress and Stress Corrosion Cracking of High Pressure Hydrocarbon Transmission Pipelines, International Pipeline Conference, Calgary Canada, 2007, 725.
20. L. Y. Xu and Y. F. Cheng, *Corros Sci.* 59 (2012) 103.
21. D. Singh and A. Kumar, A Fresh Look at ASTM G 1-90 Solution Recommended for Cleaning of Corrosion Products Formed on Iron and Steels, Corrosion -Houston Tx-, 59 (2003) 1029.
22. M. Büchler, *Mater. Corros.,* 63 (2012) 1181.
23. C. Xu and L. Chi, *Corros Sci. prot technol.*, 16 (2004) 268.
24. S. LALVANI and X. LIN, *Corros Sci.* 36 (1994) 1039.
25. S. GOIDANICH, L. LAZZARI and M. ORMELLESE, *Corros Sci.*, 52 (2010) 491.
26. S. Bordbar, M. Alizadeh and S.H. Hashemi, *Mater. Des.*, 45 (2013) 597.
27. Z. Tang, S. Hong, W. Xiao and J. Taylor, *Corros Sci.*, 48 (2006) 308.
28. N. Dai, J. Zhang and Q. Chen, *Corros Sci.*, 99 (2015) 295.
29. Y. GUO, T. Meng, D. Wang, H. Tan and R. He, *Eng Fail Anal.*,78 (2017) 87.